Polymer Bulletin 59, 527–536 (2007)
DOI 10.1007/s00289-007-0796-3

Polymer Bulletin

Structural Evolution of Polyacrylonitrile Precursor Fibers during Preoxidation and Carbonization

Minxia Ji[1, 2] (✉), Chengguo Wang[2], Yujun Bai[2], Meijie Yu[2], Yanxiang Wang[2]

[1]Key Laboratory of Liquid Structure and Heredity of Materials, Ministry of Education, Shandong University, Jinan 250061, China
[2]Carbon Fiber Engineering Research Center of Shandong Province, College of Materials Science and Engineering, Shandong University, Jinan 250061, China
E-mail: ji_minxia@163.com

Received: 13 February 2007 / Revised version: 30 May 2007 / Accepted: 31 May 2007
Published online: 19 June 2007 –

Summary

Structural evolution of polyacrylonitrile precursor fibers during preoxidation and carbonization were studied using SEM combined with XRD, FTIR, elemental analysis and density measurement. Crystallite structure of fibers has been completely changed through the process. Crystallite size of fibers firstly increases before 235°C, and then decreases with temperature increasing, whereas crystallinity gradually decreases during preoxidation. The combination between fibrils during preoxidation firstly becomes looser, and then gets denser. Meanwhile fibrils at first grow thicker, followed by getting thinner. Homogeneous and granular fracture surface of the resultant carbon fiber is obtained. Fracture morphology during the preparation undergoes transformation from ductile fracture feature to brittle fracture feature, which corresponds to changes of tensile strength and elongation at break from 0.865 GPa to 3.51 GPa, from 9.8% to 1.7%, respectively.

Introduction

Polyacrylonitrile (PAN)-based carbon fibers are now widely used as a kind of reinforcement material in the lightweight composites, because of its high strength, high elastic modulus and low density [1]. In the past decades, significant improvements in the tensile strength of carbon fibers have been achieved. At present commercial high strength carbon fibers have a maximum strength of 7.02 GPa, which, however, is only 3.9 percent of theoretical value [2]. There still seems to be a lot of room for improving the properties of carbon fibers. The key is to optimize structure which determines the properties, to get better understanding of the tensile fracture mechanism, and to find out the relationship between structure and tensile strength of fibers.

The manufacture of PAN-based carbon fibers contains three stages: spinning of PAN precursors fibers, preoxidation and carbonization. PAN precursor fibers usually need to be preoxidized under low temperature to change the linear PAN molecular chains into aromatic ladder structure which is suitable for further carbonization. With carbonization under high temperature, aromatic rings continue to condense and then convert into turbostratic graphite structure [3-4]. Thus, for fiber structure, from precursor fibers to

carbon fibers, fundamental changes have taken place. More detailed studies on fine structure of fibers throughout all processing stages are necessary, if we are to completely understand the nature of physical and mechanical property variations. However, most of the previous work was focused on the structural influence of single process on the properties of carbon fibers [5-9], and little has been done to study the structural evolution, especially the tensile fracture morphologies, throughout the whole process. Fracture surfaces of fibers exhibit morphological features related to variations in the physical properties. In this study, XRD, FTIR, SEM and some traditional testing, such as density measurement and elemental analysis were used to get deep insight into the structural evolution of PAN precursor fibers during the preoxidation and carbonization process.

Experimental

Materials

PAN precursor fibers were wet spun in dimethylsulfoxide (DMSO) with a 21 wt.% copolymer of acrylonitrile/itaconic acid (AN/IA 99/1wt.%). A self-designed continuous carbon fiber production line as shown in Figure 1, was used for thermal stabilization and subsequent carbonization of precursor fibers. The line is composed of two thermal stabilization furnaces and each has five separate temperature zones, two carbonization furnaces and eight sets of stretching equipments. The precursor fibers were preoxidized in a purified air under 5% stretching. The temperature in 10 furnace zones was designated in sequence as 195°C, 205°C, 225°C, 235°C, 245°C, 255°C, 265°C, 275°C, 275°C and 280°C, respectively. Subsequently, the oxidized fibers were subjected to low-temperature carbonization in a pure nitrogen atmosphere from 350°C to 600°C under a stretching ratio 1.5%, and to high-temperature carbonization from 1280°C to

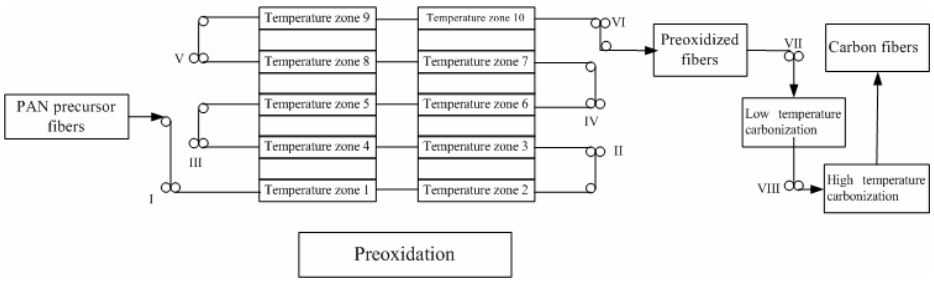

Figure 1 Scheme of carbon fiber production line with (I~VIII) stretching rollers

Table 1 Some properties of various fibers

Sample	Titre (dtex)	Tensile Strength (GPa)	Young's Modulus (GPa)	Elongation at break (%)
PAN fibers	0.98	0.865	8.82	9.80
preoxidized fibers	0.94	0.256	3.36	7.60
carbon fibers	0.50	3.51	206	1.70

1400°C under a stretching ratio 4% also in a pure nitrogen atmosphere to obtain the resulting carbon fibers. Some properties of PAN precursor fibers, preoxidized fibers and resultant carbon fibers are listed in Table 1.

Characterization

The titre of fibers at various stages was measured by a XD-1 fiber fineness machine, and mechanical properties of PAN precursor fibers, preoxidized fibers and carbon fibers were measured by a XQ-1 tensile testing machine (both XD-1 and XQ-1 were made in Donghua University, Shanghai, China) and CMT4204 tensile test machine (Shenzhen Sans Testing Machine Co., Ltd, Shenzhen, China).

The element contents in the fibers at all stages were measured by a Vario EL III elemental analyzer (Germany).

The density of various fibers was determined at 25°C by a density gradient column method. Two columns were used: one comprising a mixture of n-heptane and carbon tetrachloride, and the other comprising n-heptane and ethylene bromide.

A Rigaku D/max-rc X-ray diffractometer with Ni-filtered Cukα radiation (λ= 0.15418nm) was used to determine the structural parameters of fibers. The scanning rate is 4°/min with a scanning step of 0.02°. The crystallite size (L_c) was calculated from the Scherrer formula:

$$L_c = \frac{K\lambda}{B\cos\theta} \quad (1)$$

Where λ is the wavelength of Cu K_α X-ray, B is the full width at half the maximum intensity (FWHM) of the (100) peak at around $2\theta = 17°$ for PAN precursor fibers and preoxidized fibers, and the (002) peak at around $2\theta = 25.5°$ for carbon fibers, and K is a constant, assigned as 0.89. The crystallinity (C) of fibers is measured by Hinrichen's method [10]:

$$C = \frac{A_c}{A_a + A_c} \times 100\% \quad (2)$$

where A_c is the area under the crystalline diffraction peaks and A_a is the area of amorphous zone.

Fourier transform infrared (FTIR) measurement was conducted using KBr disks by mixing 0.5mg fibers at various stages with 200mg KBr on a Bruker Vector 22 spectrometer (America).

Fibers at various stages were impregnated with epoxy resin and cured at 100°C. Then the samples were drawn to failure by CMT4204 tensile test machine. Fracture morphologies of carbon fibers were topographically examined and photographed using JEC-560 scanning electron microscope (JEOL, Japan). Prior to examination, the specimens were coated with carbon to get a better image.

Results and Discussion

Changes of XRD structure

Figure 2 displays the X-ray diffraction (XRD) pattern of the fibers at all stages. The corresponding changes of the crystallite size and the crystallinity of fibers are tabulated

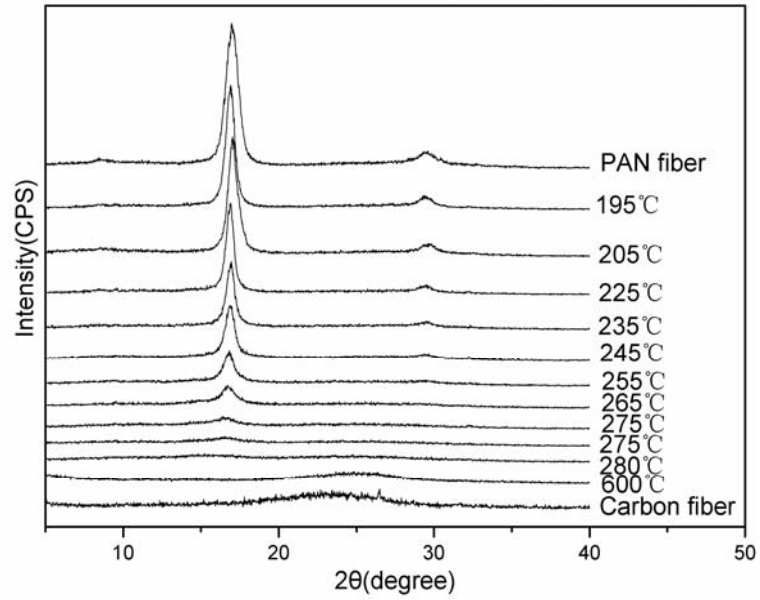

Figure 2 XRD pattern of fibers at all stages

Table 2 XRD data of fibers at all stages

Sample	Crystallite size (nm)	Crystallinity (%)
PAN fiber	8.54	58.6
195°C	12.09	54.3
205°C	11.78	53.2
225°C	13.92	47.2
235°C	13.94	45.3
245°C	11.23	42.9
255°C	10.50	32.5
265°C	7.91	30.2
275°C	5.90	18.9
275°C	5.09	—
280°C	5.06	—
600°C	1.73	—
Carbon fiber	1.76	21.8

in Table 2. Two peaks occur around 2θ=17° and 29.5° in the XRD pattern of PAN precursor fiber, representing PAN crystallite structure [11]. In the course of stabilization, the peak around 2θ=17° firstly becomes sharp with the temperature increasing due to stretching and heating, which is resulted from an increase in crystallite

size (L_c) as shown in Table 2. When the fibers were heated to higher temperatures, the intensities of these two peaks continue to weaken, suggesting a decrease in crystallinity and crystallite size, and the linear molecular chains change into aromatic ladder structure. While above 235°C, the peak around 17° decreases rapidly and finally disappears at 280°C. Meanwhile, a new wide and flat peak appears around 2θ=25.5°, demonstrating the formation of turbostratic graphite structure [12]. During carbonization, the peak around 25.5° gradually strengthens with temperature increasing. From the above results, it can be seen that structure of fibers has been completely changed through the process, which can be further confirmed by the following FTIR and fracture morphology analysis.

Changes of chemical structure

Figure 3 is the FTIR spectra of fibers at various stages. At the initial stage of preoxidation (below 235°C), the intensity of absorption peak at 2243 cm^{-1} assigned to C≡N, 2939 cm^{-1}, 1454 cm^{-1}, and 1358 cm^{-1} attributed to C–H, and band at 1070cm^{-1} assigned to C–CN gradually weaken. There is no obvious change at 1620 cm^{-1} assigned to C=C. With temperature increasing, the absorption peak at 1620 cm^{-1} begins to intensify due to dehydrogenation. Meanwhile, a shoulder at 1772 cm^{-1} attributed to C=O appears and gradually increases because of oxidation reaction [3]. At 280°C, the bands at 2243 cm^{-1}, 2939 cm^{-1}, 1454 cm^{-1}, and 1358 cm^{-1}, and 1070cm^{-1} basically disappear. Owing to the highly absorbing nature of black carbon fibers, FTIR could not give much information about chemical structure related to carbonization progress. As shown in Figure 3, the FTIR spectra of carbon fiber approach to a line. So we combine with element and density analysis to study changes of chemical structure.

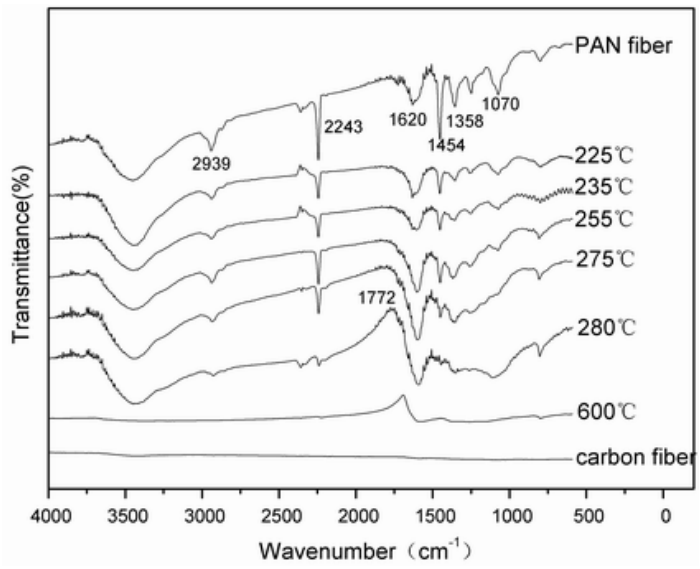

Figure 3 FTIR spectra of fibers at all stages

Figure 4 shows the changes of element contents (wt. %) during preoxidation. During the initial stage, i.e. 195°C -235°C, PAN precursor fibers mainly undergo morphological

structure rearrangements. High and adequate stretching is usually imposed in this period so as to induce additional orientation and order in the fibers. According to Figure 4, the contents of C, H and N decrease slowly, while that of O increases. Meanwhile, from Figure 5 it can be seen that the density increases slightly. Above 235°C, the content of O increases obviously along with the gradual decrease of C, H and N, and the density increases rapidly, which can be resulted from the cyclization reaction, dehydrogenation reaction and oxidation reaction. In the presence of oxygen, C≡N bonds convert into C=N bonds with the formation of ladder structure. The cohesive energy between the relative chains drops appreciably [13], which accounts for the decrease in tensile strength of preoxidized fibers as shown in Table 1. The element contents of fibers at all stages are listed in Table 3. The carbonization process results in

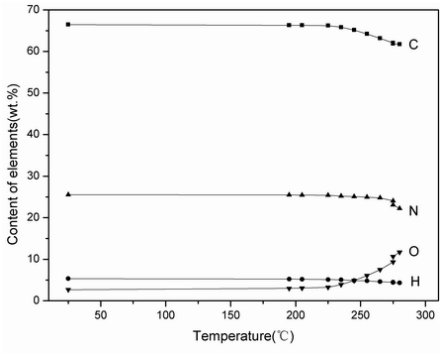

Figure 4 changes of element contents during preoxidation

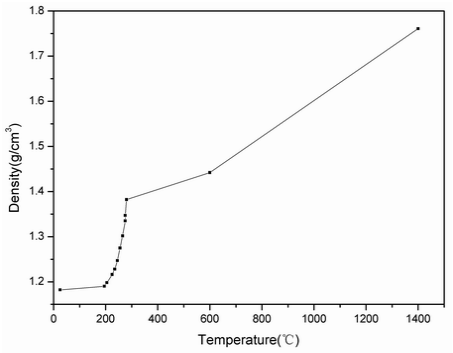

Figure 5 Changes of density at all stages

Table 3 The element contents and densities of fibers at various stages

Sample	C (wt. %)	H (wt. %)	N (wt. %)	O (wt. %)	Density (g/cm^3)
PAN fiber	66.45	5.362	25.50	2.688	1.182
195°C	66.32	5.218	25.47	2.992	1.190
205°C	66.30	5.19	25.43	3.08	1.198
225°C	66.22	5.112	25.40	3.268	1.216
235°C	65.83	5.071	25.19	3.909	1.228
245°C	65.18	4.872	25.08	4.868	1.247
255°C	64.21	4.778	24.94	6.072	1.275
265°C	63.17	4.587	24.75	7.493	1.302
275°C	62.08	4.478	24.07	9.372	1.335
275°C	61.86	4.394	23.09	10.656	1.347
280°C	61.73	4.34	22.21	11.72	1.382
600°C	66.07	3.13	19.97	10.83	1.452
Carbon fiber	94.81	0.416	4.059	0.715	1.761

cross-linking between adjacent chains. Bahl and Manocha [14] suggested that this cross-linking obtained by carbonizing the preoxidized fiber accounts for the increase in the strength of carbon fibers. During carbonization, there is a large weight loss, producing a large volume of volatile gases and some tarry substances, and the content of C increases while the O, H and N content decreases. The increase of C indicates that more basal planes are formed during carbonization, which could lead to the rearrangement and compactness of structures along the fiber axis. From Table 3 it can be seen that density increases during carbonization. As a result, carbon fiber with about 95% of C and 1.76g/cm^3 of density is obtained.

Changes of fracture morphology

As mentioned above, 235°C is a turning point of preoxidation where fiber structure begins to transform obviously, besides 255°C is also a key point where a series of physical and chemical changes occurs. In order to systemically study the evolution of fracture morphology and find out correlation between structure and mechanical properties during the preparation stages, PAN precursor fibers, fibers stabilized at 235°C, 255°C and 280°C, fibers carbonized at low temperature and the resultant carbon fibers, respectively, were selected as samples to examine their tensile fracture morphology by SEM. Figure 6 exhibits the SEM images of fracture morphology of PAN precursor fibers. Fractographs in Figure 6 (a) and (b) show typical ductile fracture features. Figure 6 (b) is a magnified image of one single filament. In the rim of the filament, protrudent fracture fibrils can be observed, demonstrating the difference of mechanical properties between the outer section and the inner section of single filament. In the transverse direction, fibrils are distributed homogeneously, and the diameter of fibrils is in the range of 200-400nm.

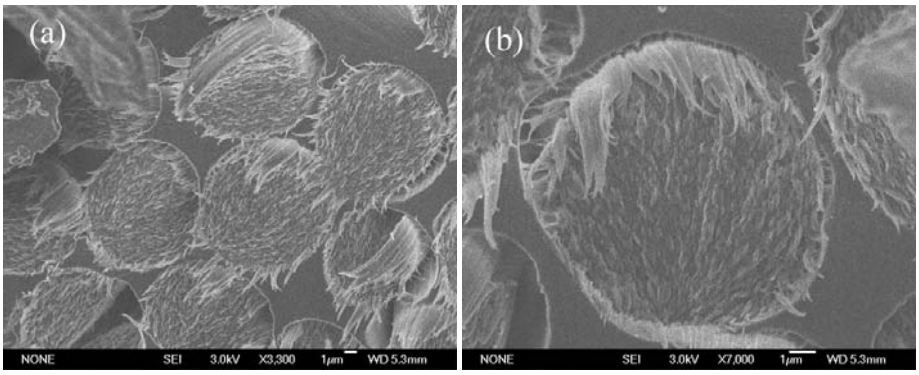

Figure 6 SEM images of fracture morphology of PAN precursor fibers

At the initial stage of preoxidation (below about 230°C), the rearrangement of PAN molecular chain segments and the initiation of cyclization reactions occur preferably in the amorphous domain. During the later stage of preoxidation (usually above 230°C), intramolecular cyclization or intermolecular crosslinking along with oxygen incorporation and dehydrogenation occurs in crystalline domain [15]. The changes of structure are demonstrated in Figure 7. Figure 7 (a) is SEM image of fracture morphology of fibers preoxidized at 235°C. It can be seen that fracture surfaces present

both ductile and brittle fracture features, which is different from PAN precursor fibers, suggesting the change of mechanical properties. From Figure 7(a), the combination between fibrils becomes looser, and the diameter of fibrils is in a range of 200-500nm which is bigger than that in Figure 6. From Figure 7 (b), the fractographs of fibers stabilized at 255°C also show both ductile and brittle fracture features. Compared with the fibers preoxidized at 235°C, fibrils become thinner with the diameter of 150-300nm and arrange more compactly. Homogeneous cross sections as shown in Figure 7 are consistent with those observed in PAN precursor fibers.

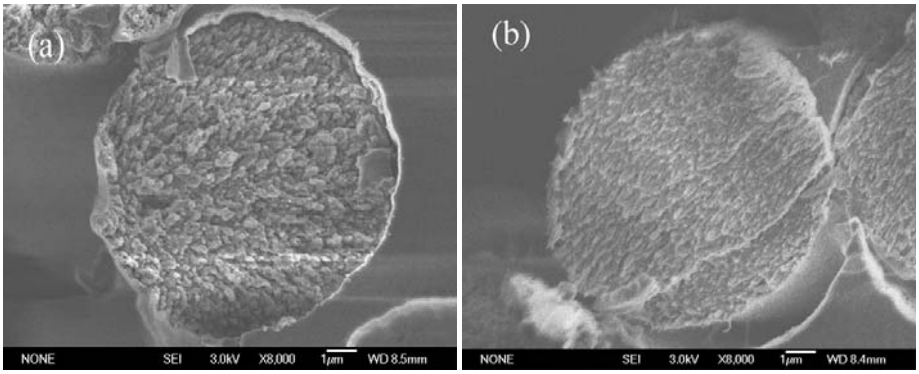

Figure 7 SEM images of fracture morphology of fibers preoxidized at (a) 235°C, and (b) 255°C

Figure 8 presents the fracture morphologies of the fibers preoxidized at 280°C, showing brittle fracture features. From Figure 8 (a), separated and grouped fibrils with diameter of 70-200nm can be observed. In the transverse direction, the fibrils distribute homogeneously, and the combination between fibrils becomes more compact than ever before. Figure 8 (b) is another SEM image of the preoxidized fiber showing step-like texture. From the image we can deduce that there are two fracture origins, which extend respectively on different plane, and finally two cracks are linked to form fracture surface owing to shear stress between two cracks.

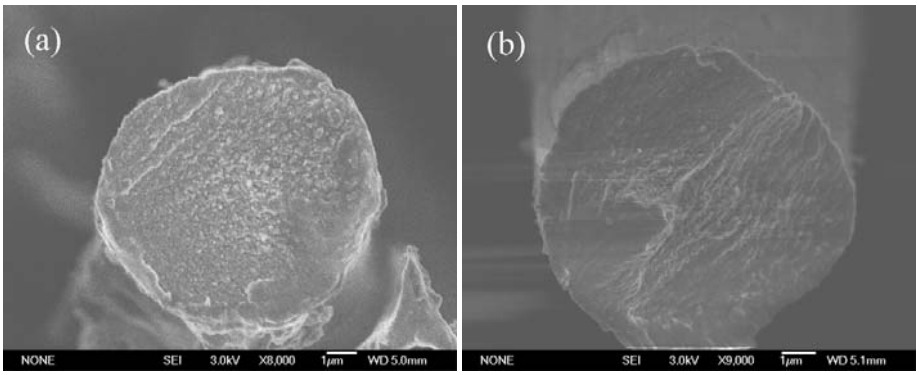

Figure 8 SEM images of fracture morphology of fibers preoxidized at 280°C

Figure 9 exhibits SEM images of fracture morphology of fibers carbonized at low temperature. The brittle fracture surface is smoother than that of the preoxidized fibers. The combination between fibrils becomes so dense that it is hard to distinguish each other. Besides homogeneous texture shown in Figure 9 (a), from Figure 9 (b), the fracture origin can be identified clearly. Beginning from one side (as marked "A" in Figure 9 (b)), the cracks are fanned out in all directions.

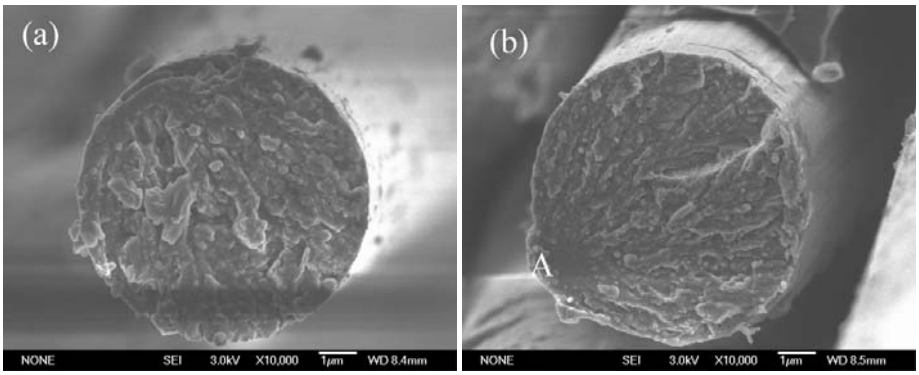

Figure 9 SEM images of fracture morphology of fibers carbonized at low temperature

Figure 10 is the SEM images of the fracture morphology of the resultant carbon fiber. According to Figure 10 (a), fibrils combine to each other, which is similar to those observed in Figure 9 (a). Figure 10 (b) is another fracture surface of carbon fiber, showing homogeneous and granular texture. The diameter of the granules is in the range of 70-200nm which accords with the diameter of fibrils [16-17], so we can conclude that granules are the fracture end of fibrils. Also from Figure 10 (b), some small voids can be observed in the surface, which partially result from volatilization of small molecular gases during high temperature carbonization. Voids should be examined as a possible source of the tensile fracture. By reducing the size and number of voids, fibrils will combine more compact, and therefore carbon fibers with fewer flaws and higher tensile strength will be obtained.

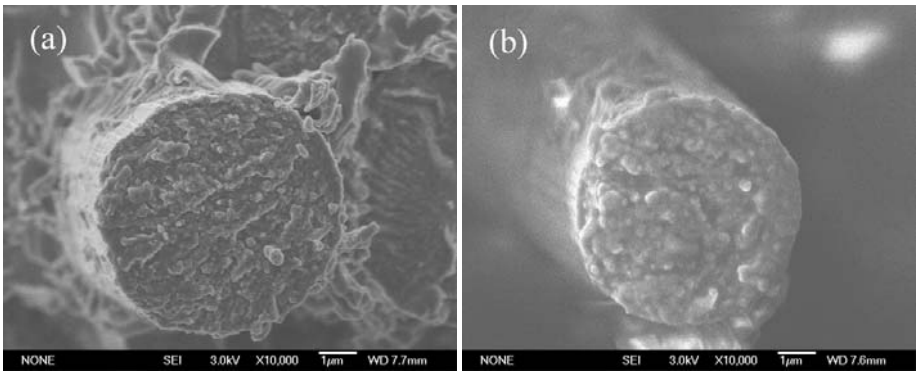

Figure 10 SEM images of fracture morphology of carbon fibers

Conclusion

In order to improve technologies to obtain perfect structure of PAN-based carbon fibers and find out relationship between structure and mechanical properties, structural evolution of fibers throughout the preparation process is studied. Mean crystallite size of fibers firstly increases below 235°C, and then decreases with temperature increasing, whereas crystallinity gradually decreases during preoxidation. Crystallite structure has been completely changes during the preparation of carbon fibers. Homogeneous texture could be observed on fracture surfaces of various fibers, and no skin-core structure is found in these specimens. Structural evolution undergoes five stages. At the initial stage of preoxidation, the combination between fibrils becomes looser, and the diameter of fibrils is bigger than that of PAN precursor fibers. At the later stage of preoxidation, fibrils become thinner and arrange more compactly. When temperature rises to 280°C, the fracture morphologies show brittle fracture features, and the combination between fibrils becomes more compact than ever before. During the low temperature carbonization, the combination between fibrils becomes so dense that it is hard to distinguish each other. At last granular fracture surface of the resultant carbon fiber is obtained. Fracture surfaces of fibers exhibit morphologic features related to variations in the physical properties. In this work, facture morphology transforms from ductile fracture feature to brittle fracture feature, which correspond to changes of tensile strength and elongation from 0.865 GPa to 3.51 GPa, from 9.8% to 1.7%, respectively.

Acknowledgements. This work was financially supported by the National Natural Science Foundation of China under grant No. 50673052 and the Major State Basic Research Development Program of China (973 Program) under grant No. 2006CB605314.

References

1. Donnet J B, Qin R Y (1993) Carbon 31: 7
2. Chand S (2000) J Mater Sci 35:1303
3. Yu MJ, Wang CG, Bai YJ, Wang YX, Wang QF, Liu HZ (2006) Polym Bull 57: 525
4. Yu MJ, Wang CG, Bai YJ, Wang YX, Xu Y (2006) Polym Bull 57: 753
5. Moreton R, Watt W (1974) Nature247:360
6. Bennett S C, Johnson D J (1983) J Mater Sci 18:3337
7. Johnson D J (1987) J Phys D (Appl Phys) 20:286
8. Huang Y, Young RJ (1995) Carbon 33: 97
9. Bai YJ, Wang CG, Lun N, Wang YX, Yu MJ, Zhu B (2006) Carbon 44: 1773
10. Hinrichsen G (1972) J Polym Sci 38: 303
11. Gupta AK, Maiti AK (1982) J Appl Polym Sci 27: 2409
12 Mukesh K J, Abhiraman A S (1987) J Mater Sci 22:278
13. Watt W, Johnson W (1975) Nature 257: 210
14. Bahl OP, Manocha LM (1974) Carbon 12: 417
15. Gupta A, Harrison IR (1996) Carbon 34: 1427
16. Johson W, Watt W (1967) Nature 215: 384
17. Guigon M, Oberline A, Desarmot G (1984) Fibre Science and Technology 20: 177